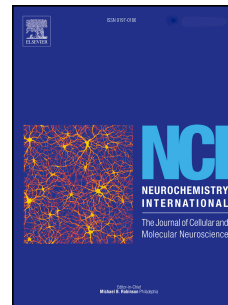


# Accepted Manuscript

Mitochondrial alterations in Parkinson's disease human samples and cellular models

Mara Zilocchi, Giovanna Finzi, Marta Lualdi, Fausto Sessa, Mauro Fasano, Tiziana Alberio



PII: S0197-0186(18)30090-1

DOI: [10.1016/j.neuint.2018.04.013](https://doi.org/10.1016/j.neuint.2018.04.013)

Reference: NCI 4238

To appear in: *Neurochemistry International*

Received Date: 27 February 2018

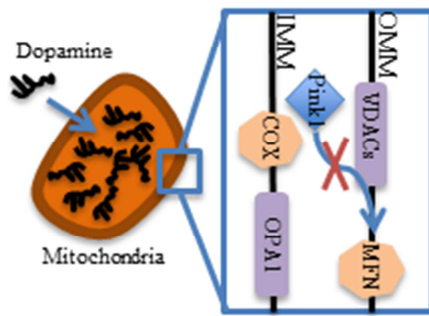
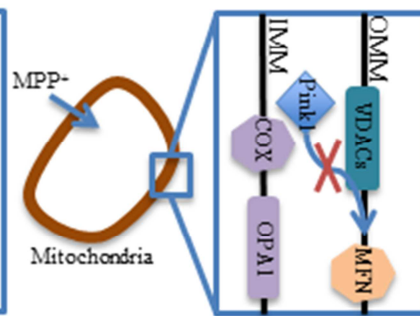
Revised Date: 16 April 2018

Accepted Date: 22 April 2018

Please cite this article as: Zilocchi, M., Finzi, G., Lualdi, M., Sessa, F., Fasano, M., Alberio, T., Mitochondrial alterations in Parkinson's disease human samples and cellular models, *Neurochemistry International* (2018), doi: 10.1016/j.neuint.2018.04.013.

This is a PDF file of an unedited manuscript that has been accepted for publication. As a service to our customers we are providing this early version of the manuscript. The manuscript will undergo copyediting, typesetting, and review of the resulting proof before it is published in its final form. Please note that during the production process errors may be discovered which could affect the content, and all legal disclaimers that apply to the journal pertain.

PD brains and dopamine:

MPP<sup>+</sup>:

ACCEPTED MANUSCRIPT

# Mitochondrial alterations in Parkinson's disease human samples and cellular models

Mara Zilocchi<sup>a</sup>, Giovanna Finzi<sup>b</sup>, Marta Lualdi<sup>a</sup>, Fausto Sessa<sup>b</sup>, Mauro Fasano<sup>a</sup>, Tiziana Alberio<sup>a\*</sup>

<sup>a</sup> Department of Science and High Technology, Center of Neuroscience, University of Insubria, Busto Arsizio 21052, Italy.

<sup>b</sup> Department of Pathology, University Hospital ASST-Settelaghi, Varese 21100, Italy.

**\* Corresponding author:**

Tiziana Alberio

Department of Science and High Technology, University of Insubria, Busto Arsizio 21052, Via Manara 7, Italy.

E-mail address: tiziana.alberio@uninsubria.it

Tel.: +39-0331-339485

**Running title:** Mitochondrial alterations in Parkinson's disease

## Abbreviations

CCCP, carbonyl cyanide 3-chlorophenylhydrazone; COX5 $\beta$ , cytochrome *c* oxidase subunit 5 $\beta$ ; DDSA, dodecenylsuccinic anhydride; DMEM, high glucose Dulbecco's modified Eagle's medium; DMP, dimethylphthalate; DMSO, dimethylsulfoxide; DRP1, dynamin-related protein 1; FBS, fetal bovine serum; FOV, field of view; IMM, inner mitochondrial membrane; MFN, mitofusin; MPP<sup>+</sup>, 1-methyl-4-phenylpyridinium; MPTP, 1-methyl-4-phenyl-1,2,3,6-tetrahydropyridine; OMA1, OMA1 zinc metallopeptidase; OMM, outer mitochondrial membrane; OPA1, optic atrophy 1; PD, Parkinson's disease; PMSF, phenylmethylsulfonyl fluoride; PINK1, PTEN-induced putative kinase 1; ROS, reactive oxygen species; TBST, tris-buffered saline with 0.05% tween 20; VDACs, voltage-dependent anion channels.

**Abstract**

Mitochondrial impairment is one of the most important hallmarks of Parkinson's disease (PD) pathogenesis. In this work, we wanted to verify the molecular basis of altered mitochondrial dynamics and disposal in Substantia nigra specimens of sporadic PD patients, by the comparison with two cellular models of PD. Indeed, SH-SY5Y cells were treated with either dopamine or 1-methyl-4-phenylpyridinium (MPP<sup>+</sup>) in order to highlight the effect of altered dopamine homeostasis and of complex I inhibition, respectively. As a result, we found that fusion impairment of the inner mitochondrial membrane is a common feature of both PD human samples and cellular models. However, the effects of dopamine and MPP<sup>+</sup> treatments resulted to be different in terms of the mitochondrial damage induced. Opposite changes in the levels of two mitochondrial protein markers (voltage-dependent anion channels (VDACs) and cytochrome *c* oxidase subunit 5 $\beta$  (COX5 $\beta$ )) were observed. In this case, dopamine treatment better recapitulated the molecular picture of patients' samples. Moreover, the accumulation of PTEN-induced putative kinase 1 (PINK1), a mitophagy marker, was not observed in both PD patients samples and cellular models. Eventually, in transmission electron microscopy images, small electron dense deposits were observed in mitochondria of PD subjects, which are uniquely reproduced in dopamine-treated cells. In conclusion, our study suggests that the mitochondrial molecular landscape of Substantia nigra specimens of PD patients can be mirrored by the impaired dopamine homeostasis cellular model, thus supporting the hypothesis that alterations in this process could be a crucial pathogenetic event in PD.

**Keywords:** Parkinson's disease; Substantia nigra; mitochondria; MPP<sup>+</sup>; dopamine.

## 1. Introduction

Parkinson's disease (PD) is a common movement disorder, with increasing prevalence in the aging population. Indeed, this pathology affects more than 1% of 65-year-old individuals and up to 5% of those over 85 years of age (Shulman *et al.*, 2011). Several biological pathways have been implicated in neuronal cell death: autophagy and mitophagy impairment, increased production of reactive oxygen species (ROS) and protein aggregation (Abdullah *et al.*, 2015; Subramaniam and Chesselet, 2013). The discovery of six responsible genes (*PARK1*, *PARK2*, *PARK6*, *PARK7*, *PARK13* and *PARK15*) that cause early-onset Parkinsonism highlighted the importance of mitochondrial dysfunction in PD pathogenesis (Burchell *et al.*, 2013; Saiki *et al.*, 2012). Altered dopamine homeostasis may be another cellular pathogenetic mechanism involved in neurodegeneration in PD (Hastings, 2009). The oxidation of dopamine at neutral pH causes the formation of endogenous toxins, which contribute to mitochondrial dysfunction and oxidative damage (Hastings, 2009; Segura-Aguilar *et al.*, 2014). It is also well known that complex I deficiency is associated to PD pathogenesis (Papa and De Rasmio, 2013; Schapira *et al.*, 1989). For this reason, the 1-methyl-4-phenyl-1,2,3,6-tetrahydropyridine (MPTP) toxin and its metabolite 1-methyl-4-phenylpyridinium (MPP<sup>+</sup>) are widely used to reproduce parkinsonian symptoms and mechanisms in animal and cellular models, respectively (Gaki and Papavassiliou, 2014; Subramaniam and Chesselet, 2013).

Mitochondria are very dynamic organelles, organized in a network constantly remodeled by fusion and fission processes (Chen and Chan, 2009; Otera and Mihara, 2011). Mitofusin 1 (MFN1) controls the fusion of the outer mitochondrial membrane (OMM), while optic atrophy 1 (OPA1) is responsible for fusion of the inner mitochondrial membrane (IMM) (Galloway *et al.*, 2012; Haroon and Vermulst, 2016; Wai and Langer, 2016). Instead, fission is mainly triggered by the cytosolic dynamin-related protein 1 (DRP1) (Galloway *et al.*, 2012; Haroon and Vermulst, 2016; Wai and Langer, 2016). In physiological conditions, in order to properly maintain the functional integrity of the mitochondrial network, a correct equilibrium between fusion and fission processes is established (Chan, 2012; Gottlieb and Bernstein, 2016) and mitochondria that are damaged are normally eliminated by a specific macroautophagic process called mitophagy (Narendra *et al.*, 2010a). When mitochondrial membrane potential is compromised, PTEN-induced putative kinase 1 (PINK1), which is usually cleaved by proteases in the IMM and subsequently degraded by the proteasome, accumulates in the OMM, thus recruiting Parkin (Narendra *et al.*, 2010a). Parkin ubiquitinates MFN1, MFN2 and other OMM proteins (e.g., voltage-dependent anion channels –VDACs), tagging mitochondria for degradation (Gegg *et al.*, 2010; Jin and Youle, 2012). At the same time, the mitochondrial

fusion is inhibited by OMA1 (Head *et al.*, 2009) and the mitochondrial fragmentation is triggered by DRP1 (Cereghetti *et al.*, 2008). These events anticipate the selective elimination of damaged mitochondria by the recruitment of the autophagosome (Dupuis, 2014). In this autophagic context, VDACs are Parkin targets and, at the same time, important for Parkin recruitment to defective mitochondria (Geisler *et al.*, 2010; Narendra *et al.*, 2010b; Sun *et al.*, 2012). Moreover, in the presence of pro-apoptotic stimuli, VDAC1 and VDAC2 are overexpressed (Naghdi and Hajnóczky, 2016; Shoshan-Barmatz *et al.*, 2008).

In the present work, we focused on the role of mitochondrial impairment in PD pathogenesis. The cellular model commonly used in our previous works, based on altered dopamine homeostasis in neuroblastoma SH-SY5Y cells, supported the hypothesis of the accumulation of dysfunctional mitochondria in cells, due to the lack of proper disposal. Thus, the permanence of depolarized mitochondria in the cell may be a leading event in PD pathogenesis (Alberio *et al.*, 2014a; Bondi *et al.*, 2016). For this reason, we investigated the main molecular factors involved in mitochondrial dynamics in other models to molecularly and mechanistically clarify the role of mitophagy impairment in PD. First, we used Substantia nigra specimens from PD patients to directly explore mitochondrial state in the tissue affected. Indeed, previous studies on autoptic brain tissues of sporadic PD patients suggested that mitochondrial impairment is clearly detectable in this type of model (Schapira *et al.*, 1990; Jenner, 2003; Bender *et al.*, 2006; Jin *et al.*, 2006; Chu *et al.*, 2014). Second, we compared results with our standard cellular model (neuroblastoma SH-SY5Y cells treated with dopamine) and with a commonly used PD cellular model (MPP<sup>+</sup> treatment). Cells exposed to carbonyl cyanide 3-chlorophenylhydrazone (CCCP) were considered as the reference cellular model for mitophagy induction.

## 2. Material and Methods

### 2.1. Cell cultures and treatments

The human neuroblastoma SH-SY5Y cell line was obtained from the European collection of cell cultures (ECACC, Cat No. 94030304; Lot No. 11C016). Cells were maintained at 37°C under humidified conditions and 5% CO<sub>2</sub> in high glucose Dulbecco's modified Eagle's medium (DMEM) (Euroclone) supplemented with 10% fetal bovine serum (FBS) (Euroclone), 100 U/mL penicillin (Euroclone), 100 g/mL streptomycin (Euroclone) and 2 mM L-glutamine (Euroclone). Cells have been used at passage number lower than 15 and were seeded at a density of  $6 \times 10^6$  per T75 flask for 24 hours before treatments. Cells were treated with 250  $\mu$ M dopamine in DMEM. 700 U/ml catalase (Sigma-Aldrich) was added to DMEM in order to

eliminate H<sub>2</sub>O<sub>2</sub> arising from extracellular dopamine auto-oxidation. The activity of complex I was inhibited using MPP<sup>+</sup> (Sigma-Aldrich) at a concentration equal to 2.5 mM in DMEM supplemented with 700 U/ml catalase. Control cells were grown in DMEM supplemented with 700 U/ml catalase.

For CCCP (Sigma-Aldrich) treatments, cells were exposed to this protonophore at a concentration of 20 μM or an equal volume of its vehicle, *i.e.*, dimethyl sulfoxide (DMSO) (Sigma-Aldrich). All treatments lasted for 24 hours.

The concentrations of MPP<sup>+</sup> and dopamine were chosen to obtain a comparable level of cell survival (60%) (Alberio *et al.*, 2014b). CCCP concentration was chosen to obtain the same cell mortality after 24 hours of treatment (data not shown).

## 2.2. Human brain specimens

Mesencephalic tissues from six sporadic PD patients and six age-matched controls (PD patients: 4 males, 2 females; mean age 73±15. Control subjects: 3 males, 3 females; mean age 72±13) were obtained from the Netherlands Brain Bank (NBB), Netherlands Institute for Neuroscience, Amsterdam (Table 1). A summary of the clinical phenotypes, neuropathological informations, and levo-dopa treatments for all PD patients is provided in the Supplementary material (Suppl. Table 1). All material has been collected from donors in the presence of a written informed consent for a brain autopsy and the use of the material and clinical information for research purposes.

This study was carried out in accordance with the recommendations of NBB with written informed consent from all subjects. All subjects gave written informed consent in accordance with the Declaration of Helsinki.

## 2.3. Western Blot Analysis

Cells were lysed in RIPA buffer (50 mM Tris-HCl pH 7.6, 150 mM NaCl, 1% sodium deoxycholate, 1% NP-40, 0.1% SDS, 1x phosphatase inhibitors (Roche), 1x protease inhibitor cocktail (Sigma-Aldrich)), incubated for 30 minutes on ice and then sonicated. Cellular lysates were then centrifuged at 15000×g for 30 minutes at 4°C.

Human brain samples were lysed by using a specific tissue lysis buffer (50 mM Tris-HCl pH 7.4, 150 mM NaCl, 1% Triton, 2 mM EDTA, 1 mM DTT, 1x phosphatase inhibitors (Roche), 1× PMSF, 1× protease inhibitor cocktail (Sigma-Aldrich)). The tissue specimens (approximately 12 mg) were put in a Potter homogenizer together with 500 μl of lysis buffer and then manually processed. After this procedure, the samples were incubated on ice for 30 minutes and then sonicated; the lysates were centrifuged at 18000×g for 15 minutes at 4°C.

Total protein concentration of both cellular and tissue lysates was quantified using the BCA method (Thermo Fisher Scientific). Equal amounts of proteins were resolved in 10% or 16% SDS-PAGE gels. Then, proteins were transferred to PVDF membranes at 1.0 mA/cm<sup>2</sup> for 1.5 hours (TE77pwr; Hoefer). Membranes were saturated for 2 hours at room temperature in tris-buffered saline with 0.05% TWEEN 20 (TBST) integrated with 5% skimmed milk powder and then incubated with primary antibody overnight at 4°C: OPA1 (HPA036927, 1:250; Sigma-Aldrich), MFN1 (sc-50330, 1:1000; Santa Cruz Biotechnology), MFN2 (HPA030554, 1:2500; Sigma-Aldrich), VDAC1 (ab15895, 1:1000; Abcam), VDAC2 (HPA043475, 1:250; Sigma-Aldrich), COX5 $\beta$  (#C4498, 1:1000; Sigma-Aldrich), PINK1 (#6946, 1:1000; Cell Signaling) or  $\beta$ -actin (GTX23280, 1 : 3000; GeneTex) in 5% milk-TBST. Incubation with proper peroxidase-conjugated secondary antibody was then performed: anti-rabbit (#AP132P, 1:1500; Millipore Corporation) and anti-mouse (#12-349, 1:3000; Millipore Corporation) in 5% milk-TBST. Enhanced chemiluminescence substrate (Millipore Corporation) was used in order to visualize the peroxidase signals: images (16 bit grayscale) were acquired using the G:BOXChemi XT4 (Syngene, Cambridge, UK) system and analyzed using the ImageJ software (Schneider *et al.*, 2012) (<https://imagej.nih.gov/ij/>). In order to quantify signal intensities of human brain lysates, the two gels were executed and transferred to PVDF simultaneously. Furthermore, the sample CTRL 99/249 was loaded in both gels to normalize signal intensities. Afterwards, signal intensities were normalized to those of  $\beta$ -actin for loading correction. For PINK1 detection in brain samples, equal amounts of proteins were resolved in 10% SDS-PAGE (SDS, TGX Stain-Free FastCast Acrylamide Kit, 10%, BioRad) and the fluorescent stain activated by UV light, following manufacturer's instructions. Then, proteins were transferred to PVDF membranes and the fluorescent signal acquired (GelDoc-It Imaging System; UVP). The total protein amount has been measured based on the total fluorescent signal in each lane with the ImageJ software.

#### **2.4. Indirect immunofluorescence**

Cells were seeded at a density of  $5 \times 10^4$  per well onto 18 mm glass coverslips in 12 multiwell plates. After 24 hours, cells were treated with MPP<sup>+</sup>, dopamine or CCCP, as described above. At the end of these treatments, cells were washed with PBS and fixed with paraformaldehyde 4% (w/v) for 15 minutes. SH-SY5Y cells were then permeabilized with Triton X-100 (0.2% in PBS) for 5 minutes and blocked with 5% FBS in PBS for 2 hours at RT. Incubation with primary antibody was performed overnight at 4°C: DRP1 (sc-32898, 1:100; Santa Cruz Biotechnology) and ATP Synthase  $\beta$  (A9728, 1:400; Sigma-Aldrich) in 5% FBS diluted in PBS. Cells were incubated with the proper Alexa Fluor 488 anti-rabbit and 647 anti-mouse



secondary antibodies (1:1000; Thermo Fisher Scientific) in 5% FBS in PBS. Coverslips were mounted with ProLong Gold Antifade mounting medium (Thermo Fisher Scientific). Images were taken with a laser-scanning confocal microscope (TCS SP5, Leica) through a 63X/1.40 NA oil-immersion objective (HCX PL APO lambda blue). All images were processed and analyzed with the ImageJ software.

The amount of DRP1 was quantified in the mitochondrial surface by choosing the most representative slices of ATP synthase  $\beta$  z-stack signals; the mitochondrial area was then selected and transposed on the corresponding z-slice of DRP1 signal in order to measure its intensity normalized on mitochondrial area. To evaluate the degree of co-localization of ATP synthase  $\beta$  and DRP1 proteins, images were transformed into 8-bit format in order to measure the Manders' Overlap Coefficient (Manders *et al.*, 1992), which expresses the amount of DRP1 signal overlapping to ATP synthase  $\beta$ , with the JaCoP plugin (Bolte and Cordelières, 2006).

## 2.5. Light and transmission electron microscopy

Mesencephalic tissues from two PD patients (07/121 and 92/080) and from two age-matched controls (09/001 and 94/325) were analysed at light and transmission electron microscopes. A section obtained from each paraffin-embedded tissue was stained with hematoxylin and eosin and examined to select the best suitable area for electron microscopy. Small fragments of paraffin-embedded brain tissues were then incubated with chloroform for 30 minutes to remove paraffin. After that, tissues were rehydrated and post-fixed with 2% Karnovsky fixative (2% paraformaldehyde and 2% glutaraldehyde in 0.05 M cacodylate buffer, pH 7.3) for two hours at 4°C, rinsed with cacodylate buffer, and eventually incubated with osmium tetroxide for one hour at room temperature. Brain tissues were then dehydrated and embedded in resin made by a mixture of araldyte, epon 812, dodecenylsuccinic anhydride (DDSA) and dimethylphthalate (DMP), whose polymerization was carried out at 60°C for 48 hours.

After treatments, SH-SY5Y cells were detached, centrifuged, washed in PBS, fixed for two hours at 4°C with 2% Karnovsky fixative, washed, post-fixed with 1% osmium tetroxide, dehydrated and embedded as previously described.

Ultrathin sections were stained with 5% uranyl acetate and Reynold's lead citrate, and observed with a Morgagni Philips/FEI transmission electron microscope.

## 2.6. Statistical analysis.

For the analysis of Substantia nigra samples, the signal of each protein was normalized to that of the sample CTRL 99/249, loaded in both gels, and then to that of  $\beta$ -actin. Data were analyzed by two-tailed, unpaired Student's t-test by comparison of Parkinson's disease patients

and control subjects.  $p < 0.05$  was considered significant.

Data obtained from control, dopamine and MPP<sup>+</sup>-treated SH-SY5Y cells were analyzed by one way ANOVA with Dunnett's post hoc test. Conversely, data obtained from DMSO- and CCCP-treated cells were analyzed by two-tailed, unpaired Student's t-test. In both cases,  $p < 0.05$  was considered significant.

For the immunofluorescence analysis, six coverslips from independent experiments were prepared for each treatment and four to five images randomly chosen were captured. The analysis of coverslips was blinded. A code number was assigned to each coverslip and the identity of the sample has been evaluated only after the software analysis of the acquired images. DRP1 and COX5 $\beta$  signal intensities were measured using ImageJ and then analyzed by two-tailed, unpaired Student's t-test.

For the analysis of TEM images, we considered several fields of view (FOVs) of the same ultra-thin section for each sample (Table 2 and Table 3). For human samples, we counted the number of total and healthy (with normal morphology) mitochondria in each cell. Moreover, we analyzed the mitochondrial damage by measuring the mitochondria with electron-dense deposits (Table 2). For SH-SY5Y cell line, we counted the number of total and healthy mitochondria (with normal morphology) (Table 3). Moreover, we counted and characterized the different mitochondrial damaged in each cell. Data obtained from control, dopamine and MPP<sup>+</sup>-treated SH-SY5Y cells were analyzed by one-way ANOVA followed by Dunnett's post hoc test. Conversely, data obtained from DMSO- and CCCP-treated cells and by human brain samples were analyzed by two-tailed, unpaired Student's t-test. In both cases,  $p < 0.05$  was considered significant. Data are presented as relative numbers, setting the value of controls (control, for dopamine and MPP<sup>+</sup> treatments; DMSO, for CCCP treatment; CTRL subjects, for PD patients) to 1, by dividing each value with the mean of the control group.

### **3. Results**

#### **3.1. Mitochondrial alterations in the Substantia nigra of PD patients**

In order to investigate molecular mitochondrial alterations occurring in the sporadic form of PD, we measured the levels of several proteins involved in mitochondrial dynamics in Substantia nigra samples obtained from five sporadic PD patients. First of all, we investigated the abundance of the two main proteins involved in mitochondrial fusion, *i.e.*, MFN1 and OPA1. As a result, we found that MFN1 did not show any difference between patients and controls (Fig. 1A). Conversely, the short form of OPA1 (OPA1-S) resulted to be decreased in

sporadic PD patients, although also the long form of this protein (OPA1-L) showed the same tendency without reaching the statistical significance (Fig. 1B).

In order to better clarify the molecular changes that occur at the mitochondrial level, we decided to measure the expression levels of VDAC1 and VDAC2, two proteins of the OMM, and of cytochrome *c* oxidase subunit 5 $\beta$  (COX5 $\beta$ ), a protein of the IMM. Protein levels of VDAC1 and VDAC2 were reduced by one half in Substantia nigra of PD patients compared to controls (Fig. 1C). On the contrary, we observed no difference in COX5 $\beta$  protein levels (Fig. 1D).

Eventually, in order to verify if these mitochondrial alterations could trigger the accumulation of PINK1 protein, the first step necessary for the activation of the PINK1/Parkin mediated-mitophagy pathway, we measured the expression level of this protein. As a result, we did not observe any PINK1 accumulation in the Substantia nigra from PD patients (Fig. 1E, Suppl. Fig. 1). CCCP-treated SH-SY5Y cells were used as positive control for PINK1 accumulation.

### 3.2. Mitochondrial alterations in dopamine and MPP<sup>+</sup>-treated SH-SY5Y cells

In order to clarify the pathological mechanisms that underlie mitochondrial dysfunction in sporadic PD patients, we decided to assess the levels of the same mitochondrial proteins in two different cellular models of PD, *i.e.*, a model of altered dopamine homeostasis (dopamine treatment) and a model of respiratory chain complex I inhibition (MPP<sup>+</sup> treatment) in SH-SY5Y cells. Moreover, cells exposed to CCCP were considered as the reference cellular model for mitophagy induction.

As a result, we found that MFN1 levels were not altered in dopamine and MPP<sup>+</sup>-treated cells, whereas they were reduced following CCCP treatment, as expected (Fig. 2A). Moreover, OPA1 protein resulted to be decreased in dopamine and MPP<sup>+</sup>-treated cells in both OPA1-L and OPA1-S forms (Fig. 2B). On the other hand, CCCP treatment caused the complete disappearance of OPA1-L and the accumulation of the pro-fission OPA1-S, as expected (Fig. 2B).

We then measured the levels of VDAC1, VDAC2 and COX5 $\beta$  proteins. Protein levels of both VDACS were significantly reduced in dopamine-treated cells, as well as after CCCP treatment. Conversely, MPP<sup>+</sup> treatment induced an increase of approximately 50% of both VDAC1 and VDAC2 proteins (Fig. 2C). On the other hand, dopamine treatment did not cause any alteration in COX5 $\beta$  protein levels. MPP<sup>+</sup> and CCCP treatments, instead, significantly decreased the levels of COX5 $\beta$  protein in SH-SY5Y cells (Fig. 2D).

Since the molecular landscape of dopamine- and MPP<sup>+</sup>-treated cells did not resemble the one obtained following CCCP treatment (*i.e.* decreased levels of all mitochondrial proteins

described above), we decided to verify the accumulation of PINK1 protein in these cellular models. As a result, we did not observe any PINK1 accumulation in dopamine and MPP<sup>+</sup>-treated cells, while it was clearly visible only following CCCP treatment, used as positive control (Fig. 2E).

In order to evaluate whether the fission process was activated following dopamine and MPP<sup>+</sup> treatments in SH-SY5Y cells, we assessed the recruitment of DRP1 to mitochondria. To this end, both quantification and co-localization of ATP synthase  $\beta$  and DRP1 protein signals were performed by immunofluorescence staining (Fig. 3A). No significant recruitment of DRP1 protein to mitochondria was observed in dopamine-treated cells. The same outcome was observed in SH-SY5Y cells treated with MPP<sup>+</sup>. By contrast, as expected, DRP1 was recruited to mitochondria following CCCP treatment, as demonstrated by both DRP1 signal quantification in the mitochondrial area (Fig. 3B) and correlation between immunofluorescence probes using the Manders' coefficient (Fig. 3C).

### **3.3. Morphological analysis of mitochondrial damage in human samples and PD cellular models**

To get a clearer vision of the differences observed in the experimental models analyzed, a morphological analysis of mitochondria was carried out by light and transmission electron microscopy. Substantia nigra sections of control and PD subjects were stained with hematoxylin and eosin and observed with a light microscope, in order to have a generic tissue characterization (Fig. 4A). An higher number of neuron cells with cytoplasmic pigments was observed in Substantia nigra sections of control subjects with respect to PD specimens, where neurons were less numerous, smaller, less pigmented, and also characterized by the presence of Lewy bodies, as expected (inset in Fig. 4A). In addition, TEM analysis demonstrated that PD neurons showed irregular nuclei and a very low number of melanin bodies (MB), if compared to control neurons (Fig. 4B). Moreover, mitochondria appeared more swollen and irregular in PD neurons, and cristae appeared to be deranged (Fig. 4C and Suppl. Fig. 2). Indeed, based on their morphology, only 17% of total mitochondria appeared to be healthy in PD patients, while the remaining 60% showed electron-dense deposits, even if the number of mitochondria per cell was not different between PD and control subjects (Fig. 4D and Table 2).

On the other hand, dopamine- and MPP<sup>+</sup>-treated SH-SY5Y cells showed abundant rough endoplasmic reticulum and Golgi cisternae, numerous mitochondria, nuclei with dispersed chromatin and nucleoli. CCCP treatment caused instead the enlargement of endoplasmic reticulum cisternae and extended vacuolization (Fig. 5A). At higher magnification (Fig. 5B), it was clear that each treatment caused a peculiar mitochondrial damage. In dopamine-treated

cells, more than 90% of mitochondria showed fusion of cristae and 70% of them displayed electron-dense deposits. In MPP<sup>+</sup>-treated cells, 90% of mitochondria appeared empty, due to a marked disruption of cristae (Fig. 5C and Table 3). Strikingly, we never observed any evident fusion between mitochondria and phagosomes in both dopamine and MPP<sup>+</sup>-treated cells, while a number of mitochondria in CCCP-treated cells appeared to be fused with phagosomes (Fig. 5D and Table 3).

#### 4. Discussion

The impairment of the mitochondrial quality control plays a central role in PD pathogenesis (Dupuis, 2014). Moreover, complex I dysfunction has been indicated as a key player in the development of this pathology (Papa and De Rasmio, 2013; Schapira *et al.*, 1989). More in general, mitochondrial dysfunction seems to be a leading event in PD (Bose and Beal 2016), although it is still unclear whether mitochondrial defects are the primary cause or a detrimental consequence of the neurodegenerative process (Polyzos and McMurray, 2017). In this work, we wanted to clarify the pathological mechanism underlying the mitochondrial impairment in PD. To this purpose, we investigated mitochondrial alterations in Substantia nigra specimens from PD patients, in comparison with three different cellular models of mitochondrial impairment in human neuroblastoma SH-SY5Y cells, obtained by: i) MPP<sup>+</sup> treatment (Langston *et al.*, 1984); ii) dopamine treatment, deeply described by our group (Alberio *et al.*, 2014a, 2014b, 2010a, 2010b; Bondi *et al.*, 2016); and iii) CCCP treatment, which is known to inhibit oxidative phosphorylation and trigger the PINK1/Parkin mitophagic pathway (Narendra *et al.*, 2010a). A comprehensive outline of the results is shown in Table 4.

First, we focused our attention on mitochondrial fusion and fission defects. Noticeably, mitochondrial fusion is typically hindered following mitochondrial damage, while the fission process is promoted, so to maintain a proper mitochondrial network assembly. Indeed, MFN1 is expected to be ubiquitinated and consequently degraded upon mitochondrial depolarization and mitophagy induction, as observed after CCCP treatment (Bondi *et al.*, 2016; Gegg *et al.*, 2010; Karbowski and Youle, 2011; Rakovic *et al.*, 2011). Nonetheless, Substantia nigra of PD patients and SH-SY5Y cells treated with MPP<sup>+</sup> or dopamine did not show significant alterations in MFN1 protein levels, thus suggesting that fusion of the OMM was not blocked. Also an impairment of the IMM fusion seemed to occur. Following the induction of the mitophagic process (*e.g.*, after CCCP treatment), what is expected to happen is the zinc metalloprotease OMA1 activation and the consequent accumulation of the short form of OPA1,

which prevents the fusion of the inner mitochondrial membranes (Head *et al.*, 2009). However, both long and short forms of OPA1 were surprisingly decreased in PD patients specimens, as well as after both MPP<sup>+</sup> and dopamine treatment in SH-SY5Y cells. This molecular event has been already related to the loss of the mitochondrial membrane integrity and in turn to the release of cytochrome *c* and apoptotic cell death (Olichon *et al.*, 2003; Ramonet *et al.*, 2013). As a matter of common knowledge, also oxidative metabolites of dopamine (*e.g.*, dopamine quinone) have been reported to inhibit complex I (Segura-Aguilar *et al.*, 2014). Thus, the impairment of the IMM fusion is a common event when complex I is inhibited, *i.e.*, in PD tissue specimens, in a cellular model of impaired dopamine homeostasis and in a cellular model of direct complex I inhibition (MPP<sup>+</sup> treatment).

DRP1 also plays a fundamental role in mitophagy and in the apoptotic process (Bossy-Wetzel *et al.*, 2003; Palikaras and Tavernarakis, 2014). We decided, therefore, to investigate the behavior of this protein in SH-SY5Y cells treated with MPP<sup>+</sup>, dopamine and CCCP. DRP1 co-localized with mitochondria only after CCCP treatment, thus suggesting that complex I inhibition or dopamine homeostasis perturbation did not cause the activation of the fission machinery. Unfortunately, this event is difficult to be verified in human tissues, where the co-localization analysis cannot be performed on the whole neuron and subcellular fractionation is hampered by the frozen nature of specimens.

We then decided to measure the levels of COX5 $\beta$ , a protein of the IMM normally used as mitochondrial marker, to have an estimate of the mitochondrial content. As mitophagy positive control, we again used the CCCP treatment, which is known to drastically reduce the number of mitochondria (Wang and Klionsky, 2011). As expected, all mitochondrial proteins analyzed (*i.e.*, MFN1, COX5 $\beta$ , VDAC1 and VDAC2) were reduced by CCCP, as a consequence of mitochondrial elimination by mitophagy. The transmission electron microscope images confirmed this view, showing the presence of many vacuoles and mitochondria fused with phagosomes. On the contrary, we did not observe any difference in mitochondrial content between PD patients and control subjects, as well as in MPP<sup>+</sup> and dopamine-treated cells with respect to controls. In line with this observation, we did not detect any difference in COX5 $\beta$  protein levels between PD patients and control subjects and the same result was obtained in SH-SY5Y cells treated with dopamine, as we previously demonstrated (Bondi *et al.*, 2016). On the other hand, COX5 $\beta$  protein level was significantly reduced after MPP<sup>+</sup> treatment, possibly reflecting the marked cristae disruption, observed by TEM.

We analyzed also the levels of the OMM VDACs proteins. Indeed, besides their role in energetic metabolism, VDACs are also involved in the regulation of calcium homeostasis and in the mitochondria-mediated apoptosis (Naghdi and Hajnóczy, 2016; Shoshan-Barmatz *et*

*et al.*, 2008). Moreover, it has been proposed that VDACs play an essential role in recruiting Parkin to defective mitochondria, in order to eliminate them through mitophagy (Geisler *et al.*, 2010; Sun *et al.*, 2012), even if their actual role in triggering this process seems to be controversial (Narendra *et al.*, 2010b). Our results showed that both VDAC1 and VDAC2 protein levels were drastically decreased in subjects with PD. VDACs were also down-regulated at the protein level after dopamine treatment (Alberio *et al.*, 2014a), probably degraded by mitochondrial proteases, as already suggested (Alberio *et al.*, 2014b; Di Pierro *et al.*, 2016). By contrast, MPP<sup>+</sup> treatment caused an increase of VDAC1 and VDAC2 proteins. Interestingly, the scenario observed in Substantia nigra specimens resembles more strictly neuroblastoma cells treated with dopamine rather than with MPP<sup>+</sup>.

Even though mitochondria are damaged, Substantia nigra of PD patients and both dopamine and MPP<sup>+</sup>-treated SH-SY5Y cells did not show any PINK1 accumulation (observed after CCCP treatment), thus suggesting that the activation of the PINK1/Parkin mitophagic pathway is impaired in both PD patients and PD cellular models. Studies conducted on the MPP<sup>+</sup> model demonstrated that the specific inhibition of complex I induced mitophagy dysfunction through a specific pathway, linked to BNIP3L degradation, decreased protein ubiquitination and p62 inactivation (Gao *et al.*, 2015; Navarro-Yepes *et al.*, 2016). Eventually, Bondi and colleagues demonstrated that dopamine treatment in SH-SY5Y cells caused an impairment of the PINK1/Parkin pathway, thus causing the accumulation of damaged mitochondria (Bondi *et al.*, 2016). Recently it has been demonstrated that the mitochondrial mass and the expression of electron transport chain proteins were not affected in the dopaminergic synapses of human PD samples. Moreover, axons of human PD Substantia nigra showed an increase in mitochondrial volumes, probably caused by an impairment in the mitophagic pathway, that may lead to an accumulation of defective mitochondria (Reeve *et al.*, 2018).

In order to better understand the molecular discrepancies observed in our models, we resorted to transmission electron microscopy (Ding *et al.*, 2012). In the MPP<sup>+</sup> treatment, we observed that 90% of mitochondria were swollen and empty. Moreover, we never observed mitochondria fused with phagosomes. This result, together with the lack of PINK1 accumulation, the unaltered number of mitochondria and the fact that the levels of OMM proteins did not decrease as happens in the CCCP model, suggests a likely impairment of mitophagy. This may lead to the accumulation of defective mitochondria, as previously demonstrated for dopamine treatment (Alberio *et al.*, 2014a). On the other hand, the treatment with dopamine determined the fusion of cristae in 90% of mitochondria. This data is in line with the reduced levels of OPA1, responsible of cristae maintenance (Ramonet *et al.*, 2013).

Moreover, some electron-dense deposits are visible inside 70% of mitochondria, representing melanized organelles, due to the entry of dopamine and the following action of dopamine-derived reactive species leading to their covalent addition to mitochondrial proteins (Alberio *et al.*, 2010b; Brenner-Lavie *et al.*, 2008; Van Laar *et al.*, 2009). Moreover, also in this case, we observed neither mitochondria fused with phagosomes nor any PINK1 accumulation, with the number of mitochondria unchanged when compared to control cells. Interestingly, also in neurons of PD subjects, mitochondria contained small electron-dense deposits. Again, what observed in Substantia nigra specimens resembles more strictly neuroblastoma cells treated with dopamine rather than with MPP<sup>+</sup>. However, TEM images from autaptic samples should be considered with caution, because of the same nature of specimens and the possible influence of fixation and conservation on their quality. Moreover, their number is often limited and they may mirror the very end of the pathogenetic process. Thus, it is not possible to establish whether mitochondria morphological alterations observed are a primary cause or just a consequence of the ongoing neurodegenerative process. Therefore, further investigation on mitophagy impairment is required.

The present study suggests that undifferentiated SH-SY5Y cells treated with dopamine represent a suitable *in vitro* model to reproduce the specific mitochondrial damage found in sporadic PD and to study neuro-protectors against this type of mitochondrial alterations. Indeed, SH-SY5Y cell line is characterized by a good activity of the dopamine transporter (DAT) and, at the same time, by a low activity of the vesicular monoamine transporter type 2 (VMAT2), thus allowing to reproduce impaired dopamine homeostasis (Alberio *et al.*, 2012; Krishna *et al.*, 2014). Defects in VMAT2 were also observed in autaptic brain tissues of PD patients (Piffl *et al.*, 2014). The importance of this vesicular transporter in PD pathology was also demonstrated in VMAT2 deficient mice that showed dopaminergic and noradrenergic neurodegeneration (Lohr *et al.*, 2017). Eventually, the accumulation of  $\alpha$ -synuclein protofibrils, a typical hallmark of sporadic PD, caused the alteration of dopamine homeostasis because of its action on DAT and VMAT2 (Bridi and Hirth, 2018).

## 5. Conclusions

To sum up, we collected several evidences that suggest that the cellular model of altered dopamine homeostasis better recapitulates the mitochondrial alterations that occur in PD patient specimens. Indeed, the molecular landscape of PD patients was similar to the one of dopamine-treated cells and also TEM images showed similar electron-dense deposits inside mitochondria. On the contrary, MPP<sup>+</sup>-treated cells were characterized by a peculiar



mitochondrial damage, *i.e.*, empty organelles, with disrupted cristae, which cannot explain the complexity of mitochondrial damage occurring in the Substantia nigra of PD patients.

Therefore, our study suggests that the acute inhibition of complex I only partially reproduces molecular mechanisms related to mitochondrial dynamics in PD, whereas dopamine-associated changes support once more the fundamental role of impaired dopamine homeostasis in PD pathogenesis.

### **Conflict of interest**

The authors declare that they have no conflict of interests.

### **Funding**

This work was supported by FAR2015 to Tiziana Alberio by Università degli Studi dell'Insubria.

### **Acknowledgments**

We thank Prof. Cristina Riva for helpful discussion.

We acknowledge the Netherlands Brain Bank for providing us the brain tissues of PD and control subjects and all the donors.

## References

- Abdullah, R., Basak, I., Patil, K.S., Alves, G., Larsen, J.P., and Møller, S.G., 2015. Parkinson's disease and age: The obvious but largely unexplored link. *Exp. Gerontol.* 68, 33-38. doi: 10.1016/j.exger.2014.09.014
- Alberio, T., Colapinto, M., Natale, M., Ravizza, R., Gariboldi, M.B., Bucci, E.M., Lopiano, L., Fasano, M., 2010a. Changes in the two-dimensional electrophoresis pattern of the Parkinson's disease related protein DJ-1 in human SH-SY5Y neuroblastoma cells after dopamine treatment. *IUBMB Life.* 62, 688-692. doi: 10.1002/iub.371
- Alberio, T., Bossi, A.M., Milli, A., Parma, E., Gariboldi, M.B., Tosi, G., Lopiano, L., Fasano, M., 2010b. Proteomic analysis of dopamine and  $\alpha$ -synuclein interplay in a cellular model of Parkinson's disease pathogenesis. *FEBS J.* 277, 4909-4919. doi: 10.1111/j.1742-4658.2010.07896.x
- Alberio, T., Lopiano, L., Fasano, M., 2012. Cellular models to investigate biochemical pathways in Parkinson's disease. *FEBS J.* 279, 1146-1155. doi: 10.1111/j.1742-4658.2012.08516.x
- Alberio, T., Mammucari, C., D'Agostino, G., Rizzuto, R., Fasano, M., 2014a. Altered dopamine homeostasis differentially affects mitochondrial voltage-dependent anion channels turnover. *Biochim. Biophys. Acta.* 1842, 1816-1822. doi: 10.1016/j.bbadis.2014.06.033
- Alberio, T., Bondi, H., Colombo, F., Alloggio, I., Pieroni, L., Urbani, A., Fasano, M., 2014b. Mitochondrial proteomics investigation of a cellular model of impaired dopamine homeostasis, an early step in Parkinson's disease pathogenesis. *Mol. Biosyst.* 10, 1332-1344. doi: 10.1039/c3mb70611g
- Bender, A., Krishnan, K.J., Morris, C.M., Taylor, G.A., Reeve, A.K., Perry, R.H., Jaros, E., Hersheson, J.S., Betts, J., Klopstock, T., Taylor, R.W., Turnbull, D.M., 2006. High levels of mitochondrial DNA deletions in substantia nigra neurons in aging and Parkinson disease. *Nat Genet.* 38, 515-517.
- Bolte, S., Cordelières, F.P., 2006. A guided tour into subcellular colocalization analysis in light microscopy. *J. Microsc.* 224, 213-232. doi: 10.1111/j.1365-2818.2006.01706.x
- Bondi, H., Zilocchi, M., Mare, M.G., D'Agostino, G., Giovannardi, S., Ambrosio, S., Fasano, M., Alberio, T., 2016. Dopamine induces mitochondrial depolarization without activating PINK1-mediated mitophagy. *J. Neurochem.* 136, 1219-1231. doi: 10.1111/jnc.13506
- Bose, A., Beal, M.F., 2016. Mitochondrial dysfunction in Parkinson's disease. *J. Neurochem.* 1,

- Bossy-Wetzell, E., Barsoum, M.J., Godzik, A., Schwarzenbacher, R., Lipton, S.A., 2003. Mitochondrial fission in apoptosis, neurodegeneration and aging. *Curr. Opin. Cell. Biol.* 15, 706-716. doi: org/10.1016/j.ceb.2003.10.015
- Braak, H., Braak, E., 1991. Neuropathological staging of Alzheimer-related changes. *Acta Neuropathol.* 82, 239-259.
- Braak, H., Bohl, J.R., Müller, C.M., Rüb, U., de Vos, R.A., Del Tredici, K., 2006. Stanley Fahn Lecture 2005: The staging procedure for the inclusion body pathology associated with sporadic Parkinson's disease reconsidered. *Mov. Disord.* 21, 2042-2051. doi: 10.1002/mds.21065
- Brenner-Lavie, H., Klein, E., Zuk, R., Gazawi, H., Ljubuncic, P., Ben-Shachar, D., 2008. Dopamine modulates mitochondrial function in viable SH-SY5Y cells possibly via its interaction with complex I: relevance to dopamine pathology in schizophrenia. *Biochim. Biophys. Acta.* 1777, 173-185. doi: 10.1016/j.bbabbio.2007.10.006
- Bridi, J.C., Hirth, F., 2018. Mechanisms of  $\alpha$ -Synuclein Induced Synaptopathy in Parkinson's Disease. *Front Neurosci.* 12, 80. doi: 10.3389/fnins.2018.00080
- Burchell, V.S., Nelson, D.E., Sanchez-Martinez, A., Delgado-Camprubi, M., Ivatt, R.M., Pogson, J.H., Randle, S.J., Wray, S., Lewis, P.A., Houlden, H., Abramov, A.Y., Hardy, J., Wood, N.W., Whitworth, A.J., Laman, H., Plun-Favreau, H., (2013). The Parkinson's disease-linked proteins Fbxo7 and Parkin interact to mediate mitophagy. *Nat. Neurosci.* 16, 1257-1265. doi: 10.1038/nn.3489
- Cereghetti, G.M., Stangherlin, A., Martins de Brito, O., Chang, C.R., Blackstone, C., Bernardi, P., Scorrano, L., (2008). Dephosphorylation by calcineurin regulates translocation of Drp1 to mitochondria. *Proc. Natl. Acad. Sci. U S A.* 105, 15803-15808. doi: 10.1073/pnas.0808249105
- Chan, D.C., 2012. Fusion and fission: interlinked processes critical for mitochondrial health. *Annu. Rev. Genet.* 46, 265-287. doi: 10.1146/annurev-genet-110410-132529
- Chen, H., Chan, D.C., 2009. Mitochondrial dynamics--fusion, fission, movement, and mitophagy in neurodegenerative diseases. *Hum. Mol. Genet.* 18, R169-176. doi: 10.1093/hmg/ddp326
- Chu, Y., Goldman, J.G., Kelly, L., He, Y., Waliczek, T., Kordower, J.H., 2014. Abnormal alpha-synuclein reduces nigral voltage-dependent anion channel 1 in sporadic and experimental Parkinson's disease. *Neurobiol Dis.* 69, 1-14. doi: 10.1016/j.nbd.2014.05.003
- Ding, W.X., Li, M., Biazik, J.M., Morgan, D.G., Guo, F., Ni, H.M., Goheen, M., Eskelinen,

- E.L., Yin, X.M., 2012. Electron microscopic analysis of a spherical mitochondrial structure. *J Biol Chem.* 287, 42373-42378. doi: 10.1074/jbc.M112.413674.
- Di Pierro, A., Bondi, H., Monti, C., Pieroni, L., Cilio, E., Urbani, A., Alberio, T., Fasano, M., Ronci, M., 2016. Experimental setup for the identification of mitochondrial protease substrates by shotgun and top-down proteomics. *EuPA Open Proteomics.* 11, 1-3. doi: org/10.1016/j.euprot.2016.02.002
- Dupuis, L., 2014. Mitochondrial quality control in neurodegenerative diseases. *Biochimie.* 100, 177-183. doi: 10.1016/j.biochi.2013.07.033
- Gaki, G.S., Papavassiliou, A.G., 2014. Oxidative stress-induced signaling pathways implicated in the pathogenesis of Parkinson's disease. *Neuromolecular Med.* 16, 217-230. doi: 10.1007/s12017-014-8294-x
- Galloway, C.A., Lee, H., Yoon, Y., 2012. Mitochondrial morphology emerging role in bioenergetics. *Free Radic. Biol. Med.* 53, 2218-2228. doi: 10.1016/j.freeradbiomed.2012.09.035
- Gao, F., Chen, D., Si, J., Hu, Q., Qin, Z., Fang, M., Wang, G., 2015. The mitochondrial protein BNIP3L is the substrate of PARK2 and mediates mitophagy in PINK1/PARK2 pathway. *Hum Mol Genet.* 24, 2528-2538. doi: 10.1093/hmg/ddv017.
- Gegg, M.E., Cooper, J.M., Chau, K.Y., Rojo, M., Schapira, A.H., Taanman, J.W., 2010. Mitofusin 1 and mitofusin 2 are ubiquitinated in a PINK1/parkin-dependent manner upon induction of mitophagy. *Hum. Mol. Genet.* 19, 4861-4870. doi: 10.1093/hmg/ddq419
- Geisler, S., Holmström, K.M., Skujat, D., Fiesel, F.C., Rothfuss, O.C., Kahle, P.J., Springer, W., 2010. PINK1/Parkin-mediated mitophagy is dependent on VDAC1 and p62/SQSTM1. *Nat. Cell. Biol.* 12, 119-131. doi: 10.1038/ncb2012
- Gottlieb, R.A., Bernstein, D., 2016. Mitochondrial remodeling: Rearranging, recycling, and reprogramming. *Cell. Calcium.* 60, 88-101. doi: 10.1016/j.ceca.2016.04.006
- Haroon, S., Vermulst, M., 2016. Linking mitochondrial dynamics to mitochondrial protein quality control. *Curr. Opin. Genet. Dev.* 38, 68-74. doi: 10.1016/j.gde.2016.04.004
- Hastings, T.G., 2009. The role of dopamine oxidation in mitochondrial dysfunction: implications for Parkinson's disease. *J. Bioenerg. Biomembr.* 41, 469-472. doi: 10.1007/s10863-009-9257-z
- Head, B., Griparic, L., Amiri, M., Gandre-Babbe, S., van der Blik, A.M., 2009. Inducible proteolytic inactivation of OPA1 mediated by the OMA1 protease in mammalian cells. *J. Cell. Biol.* 187, 959-966. doi: 10.1083/jcb.200906083

- Jenner, P., 2003. Oxidative stress in Parkinson's disease. *Ann. Neurol.* 53 Suppl 3, S26-36. doi: [10.1002/ana.10483](https://doi.org/10.1002/ana.10483)
- Jin, J., Hulette, C., Wang, Y., Zhang, T., Pan, C., Wadhwa, R., Zhang, J., 2006. Proteomic identification of a stress protein, mortalin/mthsp70/GRP75: relevance to Parkinson disease. *Mol Cell Proteomics.* 5:1193-1204.
- Jin, S.M., Youle, R.J., 2012. PINK1 and Parkin-mediated mitophagy at a glance. *J. Cell. Sci.* 125, 795-799. doi: [10.1242/jcs.093849](https://doi.org/10.1242/jcs.093849)
- Karbowski, M., Youle, R.J., 2011. Regulating mitochondrial outer membrane proteins by ubiquitination and proteasomal degradation. *Curr. Opin. Cell. Biol.* 23, 476-482. doi: [10.1016/j.ceb.2011.05.007](https://doi.org/10.1016/j.ceb.2011.05.007)
- Krishna, A., Biryukov, M., Trefois, C., Antony, P.M., Hussong, R., Lin, J., Heinäniemi, M., Glusman, G., Köglsberger, S., Boyd, O., van den Berg, B.H., Linke, D., Huang, D., Wang, K., Hood, L., Tholey, A., Schneider, R., Galas, D.J., Balling, R., May, P., 2014. Systems genomics evaluation of the SH-SY5Y neuroblastoma cell line as a model for Parkinson's disease. *BMC Genomics.* 15, 1154. doi: [10.1186/1471-2164-15-1154](https://doi.org/10.1186/1471-2164-15-1154)
- Langston, J.W., Irwin, I., Langston, E.B., Forno, L.S., 1984. 1-Methyl-4-phenylpyridinium ion (MPP<sup>+</sup>): identification of a metabolite of MPTP, a toxin selective to the substantia nigra. *Neurosci. Lett.* 48, 87-9. doi: [org/10.1016/0304-3940\(84\)90293-3](https://doi.org/10.1016/0304-3940(84)90293-3)
- Lohr, K.M., Masoud, S.T., Salahpour, A., Miller, G.W., 2017. Membrane transporters as mediators of synaptic dopamine dynamics: implications for disease. *Eur J Neurosci.* 45:20-33. doi: [10.1111/ejn.13357](https://doi.org/10.1111/ejn.13357).
- Manders, E.M., Stap, J., Brakenhoff, G.J., van Driel, R., Aten, J.A., 1992. Dynamics of three-dimensional replication patterns during the S-phase, analysed by double labelling of DNA and confocal microscopy. *J. Cell. Sci.* 103, 857-862.
- Naghdi, S., Hajnóczky, G., 2016. VDAC2-specific cellular functions and the underlying structure. *Biochim. Biophys. Acta.* 1863, 2503-2514. doi: [10.1016/j.bbamcr.2016.04.020](https://doi.org/10.1016/j.bbamcr.2016.04.020)
- Narendra, D.P., Jin, S.M., Tanaka, A., Suen, D.F., Gautier, C.A., Shen, J., Cookson, M.R., Youle, R.J., 2010a. PINK1 is selectively stabilized on impaired mitochondria to activate Parkin. *PLoS Biol.* 8, e1000298. doi: [10.1371/journal.pbio.1000298](https://doi.org/10.1371/journal.pbio.1000298)
- Narendra, D., Kane, L.A., Hauser, D.N., Fearnley, I.M., Youle, R.J., 2010b. p62/SQSTM1 is required for Parkin-induced mitochondrial clustering but not mitophagy; VDAC1 is dispensable for both. *Autophagy.* 6, 1090-1106. doi: [10.4161/auto.6.8.13426](https://doi.org/10.4161/auto.6.8.13426)
- Navarro-Yepes, J., Anandhan, A., Bradley, E., Bohovych, I., Yarabe, B., de Jong, A., Ovaa, H., Zhou, Y., Khalimonchuk, O., Quintanilla-Vega, B., Franco, R., 2016. Inhibition of

- Protein Ubiquitination by Paraquat and 1-Methyl-4-Phenylpyridinium Impairs Ubiquitin-Dependent Protein Degradation Pathways. *Mol Neurobiol.* 53, 5229-5251. doi: 10.1007/s12035-015-9414-9
- Olichon, A., Baricault, L., Gas, N., Guillou, E., Valette, A., Belenguer, P., Lenaers, G., 2003. Loss of OPA1 perturbs the mitochondrial inner membrane structure and integrity, leading to cytochrome c release and apoptosis. *J. Biol. Chem.* 278, 7743-7746. doi: 10.1074/jbc.C200677200
- Otera, H., Mihara, K., 2011. Molecular mechanisms and physiologic functions of mitochondrial dynamics. *J. Biochem.* 149, 241-251. doi: 10.1093/jb/mvr002
- Palikaras, K., Tavernarakis, N., 2014. Mitochondrial homeostasis: the interplay between mitophagy and mitochondrial biogenesis. *Exp. Gerontol.* 56, 182-188. doi: 10.1016/j.exger.2014.01.021
- Papa, S., De Rasmio, D., 2013. Complex I deficiencies in neurological disorders. *Trends. Mol. Med.* 19, 61-69. doi: 10.1016/j.molmed.2012.11.005
- Pifl, C., Rajput, A., Reither, H., Blesa, J., Cavada, C., Obeso, J.A., Rajput, A.H., Hornykiewicz, O., 2014. Is Parkinson's disease a vesicular dopamine storage disorder? Evidence from a study in isolated synaptic vesicles of human and nonhuman primate striatum. *J Neurosci.* 34, 8210-8218. doi: 10.1523/JNEUROSCI.5456-13.2014
- Polyzos, A.A., McMurray, C.T., 2017 The chicken or the egg: mitochondrial dysfunction as a cause or consequence of toxicity in Huntington's disease. *Mech. Ageing.* 161, 181-197. doi: 10.1016/j.mad.2016.09.003
- Rakovic, A., Grünewald, A., Kottwitz, J., Brüggemann, N., Pramstaller, P.P., Lohmann, K., Klein, C., 2011. Mutations in PINK1 and Parkin impair ubiquitination of Mitofusins in human fibroblasts. *PLoS One.* 6, e16746. doi: 10.1371/journal.pone.0016746
- Ramonet, D., Perier, C., Recasens, A., Dehay, B., Bové, J., Costa, V., Scorrano, L., Vila, M., 2013. Optic atrophy 1 mediates mitochondria remodeling and dopaminergic neurodegeneration linked to complex I deficiency. *Cell Death Differ.* 20, 77-85. doi: 10.1038/cdd.2012.95
- Reeve, A.K., Grady, J.P., Cosgrave, E.M., Bennison, E., Chen, C., Hepplewhite, P.D., Morris, C.M., 2018. Mitochondrial dysfunction within the synapses of substantia nigra neurons in Parkinson's disease. *npj Parkinson's Disease.* 4, 9. doi:10.1038/s41531-018-0044-6
- Saiki, S., Sato, S., Hattori, N., 2012. Molecular pathogenesis of Parkinson's disease: update. *J. Neurol. Neurosurg. Psychiatry.* 83, 430-436. doi: 10.1136/jnnp-2011-301205
- Schapira, A.H., Cooper, J.M., Dexter, D., Jenner, P., Clark, J.B., Marsden, C.D., 1989. Mitochondrial complex I deficiency in Parkinson's disease. *Lancet.* 1, 1269

- Schapira, A.H., Cooper, J.M., Dexter, D., Clark, J.B., Jenner, P., Marsden, C.D., 1990. Mitochondrial complex I deficiency in Parkinson's disease. *J Neurochem.* 54, 823-827.
- Schneider, C.A., Rasband, W.S., Eliceiri, K.W., 2012. NIH Image to ImageJ: 25 years of image analysis. *Nat. Methods.* 9, 671-675. doi:10.1038/nmeth.2089
- Segura-Aguilar, J., Paris, I., Muñoz, P., Ferrari, E., Zecca, L., Zucca, F.A., 2014. Protective and toxic roles of dopamine in Parkinson's disease. *J. Neurochem.* 129, 898-915. doi: 10.1111/jnc.12686
- Shoshan-Barmatz, V., Keinan, N., Zaid, H., 2008. Uncovering the role of VDAC in the regulation of cell life and death. *J. Bioenerg. Biomembr.* 40, 183-191. doi: 10.1007/s10863-008-9147-9
- Shulman, J.M., De Jager, P.L., Feany, M.B., 2011. Parkinson's disease: genetics and pathogenesis. *Annu. Rev. Pathol.* 6, 193-222. doi: 10.1146/annurev-pathol-011110-130242
- Subramaniam, S.R., Chesselet, M.F., 2013. Mitochondrial dysfunction and oxidative stress in Parkinson's disease. *Prog. Neurobiol.* 106-107, 17-32. doi: 10.1016/j.pneurobio.2013.04.004
- Sun, Y., Vashisht, A.A., Tchieu, J., Wohlschlegel, J.A., Dreier, L., 2012. Voltage-dependent anion channels (VDACs) recruit Parkin to defective mitochondria to promote mitochondrial autophagy. *J. Biol. Chem.* 287, 40652-40660. doi: 10.1074/jbc.M112.419721
- Thal, D.R., Rüb, U., Schultz, C., Sassin, I., Ghebremedhin, E., Del Tredici, K., Braak, E., Braak, H., 2000. Sequence of Abeta-protein deposition in the human medial temporal lobe. *J. Neuropathol. Exp. Neurol.* 59, 733-748.
- Tudorache, I.F., Trusca, V.G., Gafencu, A.V., 2017. Apolipoprotein E - A Multifunctional Protein with Implications in Various Pathologies as a Result of Its Structural Features. *Comput Struct Biotechnol J.* 15, 359-365. doi: 10.1016/j.csbj.2017.05.003.
- Van Laar, V.S., Mishizen, A.J., Cascio, M., Hastings, T.G., 2009. Proteomic identification of dopamine-conjugated proteins from isolated rat brain mitochondria and SH-SY5Y cells. *Neurobiol. Dis.* 34, 487-500. doi: 10.1016/j.nbd.2009.03.004
- Wai, T., Langer, T., 2016. Mitochondrial Dynamics and Metabolic Regulation. *Trends. Endocrinol. Metab.* 27, 105-117. doi: 10.1016/j.tem.2015.12.001
- Wang, K., Klionsky, D.J., 2011. Mitochondria removal by autophagy. *Autophagy.* 7, 297-300. doi: 10.4161/auto.7.3.14502

## Captions to the Figures

- Fig. 1.** Proteins involved in mitochondrial dynamics in the Substantia nigra of PD patients. Representative Western blot images (left) in the Substantia nigra of PD patients (PD) and control subjects (CTRL) and relative protein level, expressed as mean  $\pm$  SEM (n = 5 control subjects and 5 PD patients in 3 technical replicates). (A) MFN1 protein level (B) OPA1 long (OPA1-L) and short (OPA1-S) forms level (C) VDAC1 and VDAC2 protein levels (D) COX5 $\beta$  protein level (E) PINK1 representative Western blot. CCCP-treated SH-SY5Y cells are used as control. Normalization was performed on total protein loading (Suppl. Fig. 1). Data were analyzed by two-tailed, unpaired Student's t-test by comparison of PD patients and CTRL subjects. \* p < 0.05
- Fig. 2.** Proteins involved in mitochondrial dynamics in dopamine, MPP<sup>+</sup>-and CCCP-treated SH-SY5Y cells. Representative Western blot images (left) and relative protein levels (right), expressed as mean  $\pm$  SEM (n = 3 to 5 biological replicates). (A) MFN1 protein level (B) OPA1 long (OPA1-L) and short (OPA1-S) forms level (C) VDAC1 and VDAC2 protein levels (D) COX5 $\beta$  protein level (E) PINK1 representative Western blot. Data obtained from control, dopamine and MPP<sup>+</sup>-treated cells were analyzed by one way ANOVA with Dunnett's post hoc test. # p < 0.05 ; ## p < 0.01; ### p < 0.001 Data were analyzed by two-tailed, unpaired Student's t-test in the comparison of CCCP and DMSO-treated cells. \* p < 0.05 ; \*\* p < 0.01; \*\*\* p < 0.001
- Fig. 3.** DRP1 is not recruited to mitochondria after dopamine or MPP<sup>+</sup> treatment. (A) Representative immunofluorescence images of ATP synthase  $\beta$  (used as mitochondrial marker), DRP1 and their overlap (scale bar: 20  $\mu$ m). (B) DRP1 signal quantification in the mitochondrial area. (C) Correlation between immunofluorescence probes using the Manders' coefficient. Data are expressed as mean  $\pm$  SEM (n = 6 biological replicates). Data obtained from control, dopamine and MPP<sup>+</sup>-treated cells were analyzed by one way ANOVA with Dunnett's post hoc test. Data of DMSO and CCCP treated cells were analyzed by two-tailed, unpaired Student's t-test. \*\*\* p < 0.001



**Fig. 4.** Mitochondrial alterations in Substantia nigra of PD patients. **(A)** Representative light microscopy images of Substantia nigra of one control subject and one PD patient stained with hematoxylin and eosin (magnification: 40X and inset 200X). A Lewy body is visible in the cytoplasm of a neuron (200X, arrow). **(B)** Representative transmission electron microscopy images of Substantia nigra neurons of one control subject and one PD patient (scale bar: 5  $\mu$ m). N: nuclei; MB: melanin bodies. **(C)** Representative transmission electron microscopy images of the same Substantia nigra neurons taken at higher magnification (scale bar: 1  $\mu$ m). Arrows indicate mitochondria. **(D)** Relative number of mitochondria, relative number of healthy mitochondria and mitochondria with electron-dense deposits. Analysis of TEM images was performed on 2 PD patients (07/121 and 92/080) and on 2 CTRL subjects (09/001 and 94/ 325). Data, expressed as mean  $\pm$  SEM, were analyzed by two-tailed, unpaired Student's t-test by comparison of PD patients and CTRL subjects. \*  $p < 0.05$  ; \*\*  $p < 0.01$

**Fig. 5.** Dopamine and MPP<sup>+</sup> treatments cause different morphological changes at the mitochondrial level. **(A)** Representative transmission electron microscopy images of dopamine-, MPP<sup>+</sup>- and CCCP- treated SH-SY5Y cells. Scale bar: 2  $\mu$ m. **(B)** Representative transmission electron microscopy images of dopamine-, MPP<sup>+</sup>- and CCCP- treated SH-SY5Y cells. Scale bar: 0.5  $\mu$ m. Arrows indicate mitochondria. In CCCP-treated cells a mitochondrion is fused with a phagosome (P). R: rough endoplasmic reticulum; G: Golgi apparatus; N: nuclei; V: vacuole. **(C)** Relative number of mitochondria, healthy mitochondria and damaged mitochondria dopamine- and MPP<sup>+</sup>- treated SH-SY5Y cells (mitochondria considered as damaged: dopamine, mitochondria with fused cristae and with electron-dense deposits; MPP<sup>+</sup>, empty mitochondria. In the control cells, mitochondria with partial derangement of cristae were considered as damaged). Data, expressed as mean  $\pm$  SEM, were analysed by one way ANOVA with Dunnett's post hoc test. ###  $p < 0.001$ . **(D)** Relative number of mitochondria, healthy mitochondria and damaged mitochondria (swollen, with derangement of cristae) in CCCP-treated SH-SY5Y cells. Data, expressed as mean  $\pm$  SEM, were analysed by two-tailed, unpaired Student's t-test. \*\*  $p < 0.01$ ; \*\*\*  $p < 0.001$

ACCEPTED MANUSCRIPT

**Table 1** Outline of Substantia nigra specimens from Parkinson's disease patients and control subjects.

<b>NBB<sup>a</sup> number</b>	<b>Autopsy number</b>	<b>Sample type</b>	<b>Braak Stage (Tau/amyloid)<sup>b</sup></b>	<b>Braak Stage LB<sup>c</sup></b>	<b>Pmd<sup>d</sup> (hr:min)</b>	<b>Brain Weight (g)</b>	<b>ApoE<sup>e</sup></b>	<b>Diagnosis</b>
2007-013	07/055	Frozen	1 O	-	07:35	1696	32	PD <sup>f</sup>
2007-029	07/121	Paraffin/Frozen	1 O	6	04:55	1217	32	PD
2006-062	06/191	Frozen	1 B	5	03:40	1155	32	PD
2009-045	09/146	Frozen	1 A	4	09:35	1440	-	PD
2009-078	09/254	Frozen	-	6	04:15	1130	-	PD
1992-035	92/080	Paraffin	0 B	5	04:15	1194	43	PD
2009-003	09/007	Frozen	1 O	0	07:20	1520	-	NDC <sup>g</sup>
1999-116	99/249	Frozen	0 O	-	04:20	1300	33	NDC
2009-001	09/001	Paraffin/Frozen	2 A	-	04:43	1418	-	NDC
2001-004	01/016	Frozen	0 B	-	08:35	1159	42	NDC
1999-111	99/232	Frozen	3 B	-	05:40	1034	33	NDC
1994-119	94/325	Paraffin	-	-	07:40	1131	33	NDC

Notes: <sup>a</sup>NBB: Netherlands Brain Bank; <sup>b</sup>Braak stage (Tau/amyloid): this is a scale for Alzheimer's pathology (Braak and Braak, 1991; Thal *et al.*, 2000); <sup>c</sup>Braak stage LB: this is a scale for Parkinson's disease (Braak *et al.*, 2006); <sup>d</sup>Pmd: postmortem delay; <sup>e</sup>ApoE: ApoE genotype (Tudorache *et al.*, 2017); <sup>f</sup>PD: Parkinson's disease; <sup>g</sup>NDC: non-demented control.

**Table 2** Morphological analysis of mitochondria in Substantia nigra samples from control subjects (CTRL) and Parkinson's disease patients (PD).

	<b>Mitochondria Counts</b>			
	<b>tot</b>	<b>per cell</b>	<b>healthy</b>	<b>with electron dense deposits</b>
<b>CTRL (*n=13)</b>	<b>107</b>	<b>8.23</b>	<b>64 (59.81%)</b>	<b>39 out of 107 (36.45%)</b>
<b>PD (*n=16)</b>	<b>143</b>	<b>8.94</b>	<b>25 (17.48%)</b>	<b>83 out of 143 (58.04%)</b>

Notes: \*n: number of cells analyzed (one cell per each field of view)

**Table 3** Morphological analysis of mitochondria in control and dopamine, MPP<sup>+</sup> or CCCP-treated SH-SY5Y cells.

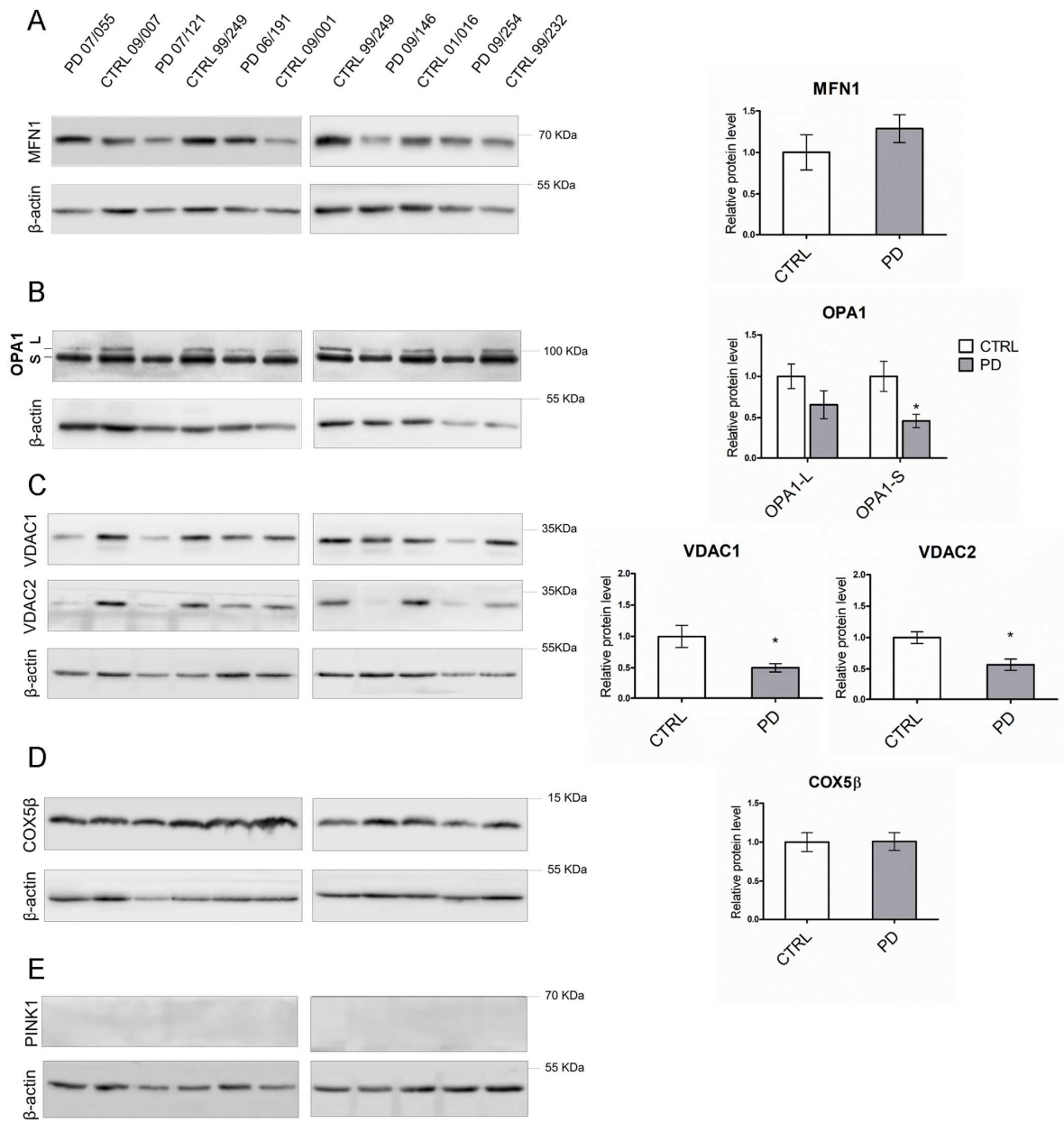
	Mitochondria Counts						
	tot	per cell	healthy	empty	with deranged cristae	with electron dense deposits	phagosome-fused
<b>Control (*n=6)</b>	<b>62</b>	<b>10.34</b>	<b>57 (91.94%)</b>	<b>NA</b>	<b>5 (8.06%)</b>	<b>NA</b>	<b>NA</b>
<b>Dopamine (*n=8)</b>	<b>73</b>	<b>9.13</b>	<b>7 (9.59%)</b>	<b>NA</b>	<b>66 (90.41%)</b>	<b>49 (67.12%)</b>	<b>NA</b>
<b>MPP<sup>+</sup> (*n=7)</b>	<b>59</b>	<b>8.43</b>	<b>6 (10.17%)</b>	<b>53 (89.83%)</b>	<b>NA</b>	<b>NA</b>	<b>NA</b>
<b>DMSO (*n=6)</b>	<b>66</b>	<b>11</b>	<b>62 (93.94%)</b>	<b>NA</b>	<b>4 (6.06%)</b>	<b>NA</b>	<b>NA</b>
<b>CCCP (*n=8)</b>	<b>52</b>	<b>6.5</b>	<b>4 (7.69%)</b>	<b>NA</b>	<b>48 (92.31%)</b>	<b>NA</b>	<b>10 (19.23%)</b>

Notes: \*n: number of cells analyzed (one cell per each field of view)

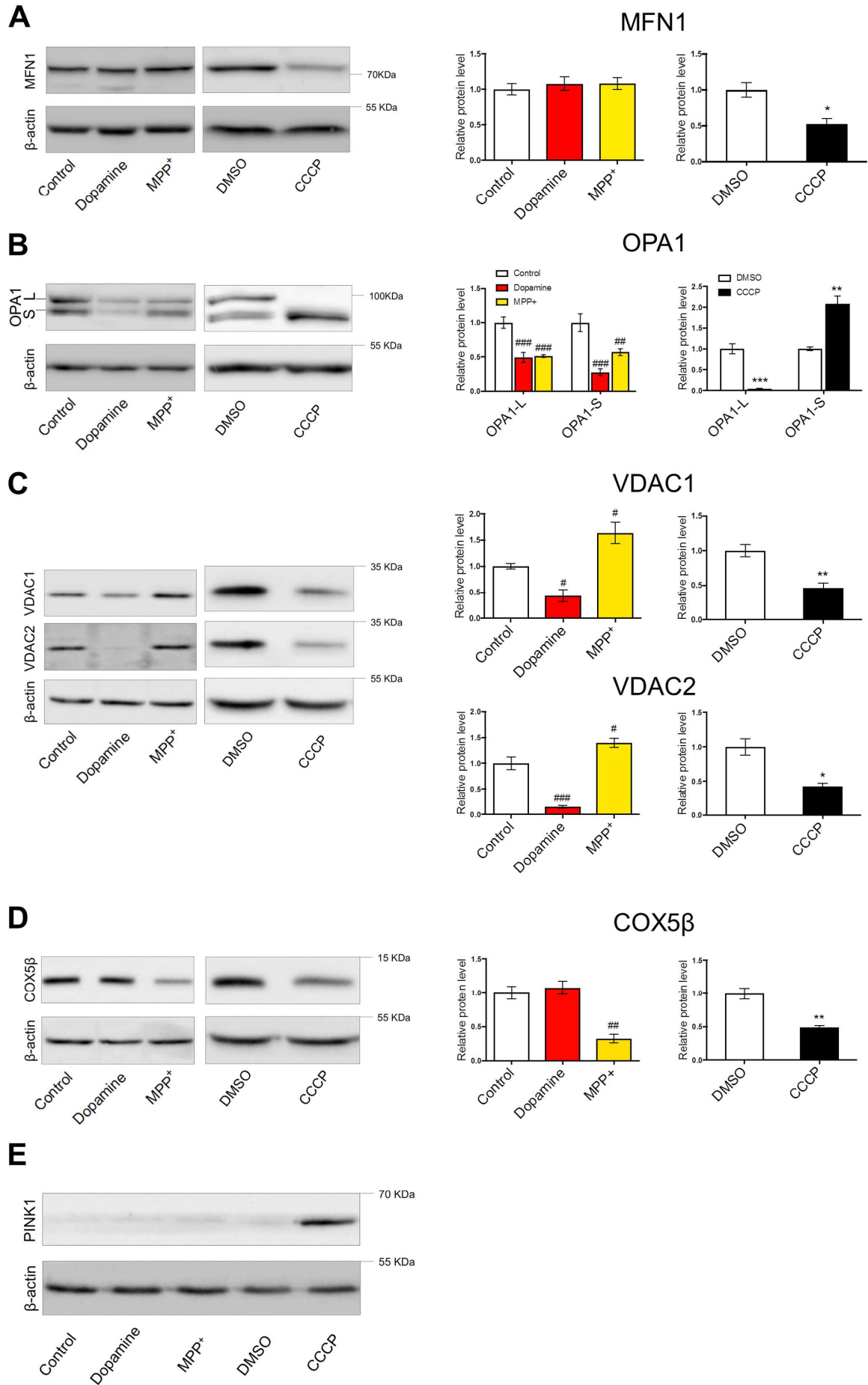
**Table 4** Results Outline

		PD Substantia nigra	SH-SY5Y		
			Dopamine	MPP <sup>+</sup>	CCCP
WB	MFN1	= <sup>a</sup>	=	=	↓ <sup>b</sup>
	OPA1-L	(↓) <sup>c</sup>	↓	↓	↓
	OPA1-S	↓	↓	↓	↑ <sup>d</sup>
	PINK1	No accumulation	No accumulation	No accumulation	Accumulation
	VDAC1	↓	↓	↑	↓
	VDAC2	↓	↓	↑	↓
	COX5β	=	=	↓	↓
IIF	DRP1 (intensity)	Not measured	=	=	↑
	DRP1 (relocalization to mitochondria)	Not measured	=	=	↑

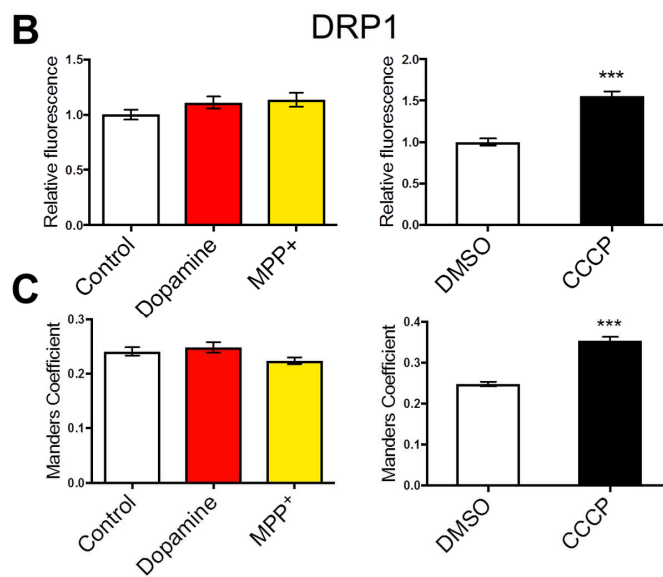
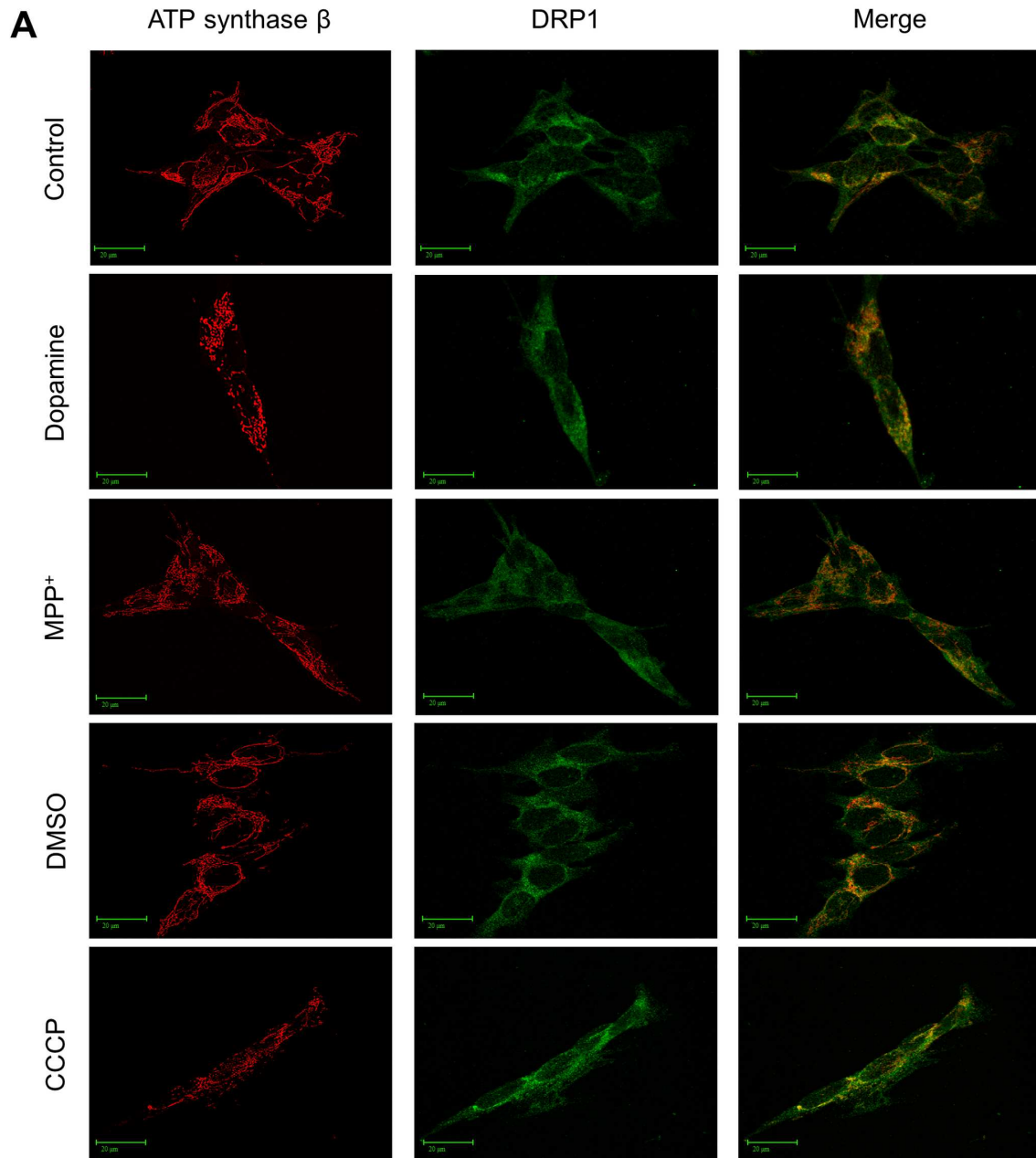
Notes: <sup>a</sup> = : protein levels are unchanged when compared to their respective controls (CTRL, for PD patients; Control, for dopamine and MPP<sup>+</sup>-treated cells; DMSO, for CCCP treatment); <sup>b</sup> ↓ : protein levels are reduced; <sup>c</sup> ( ↓ ) : protein levels seems to be reduced without reaching statistical significance; <sup>d</sup> ↑ : protein levels are increased. WB: Western blot; IIF: Indirect ImmunoFluorescence.

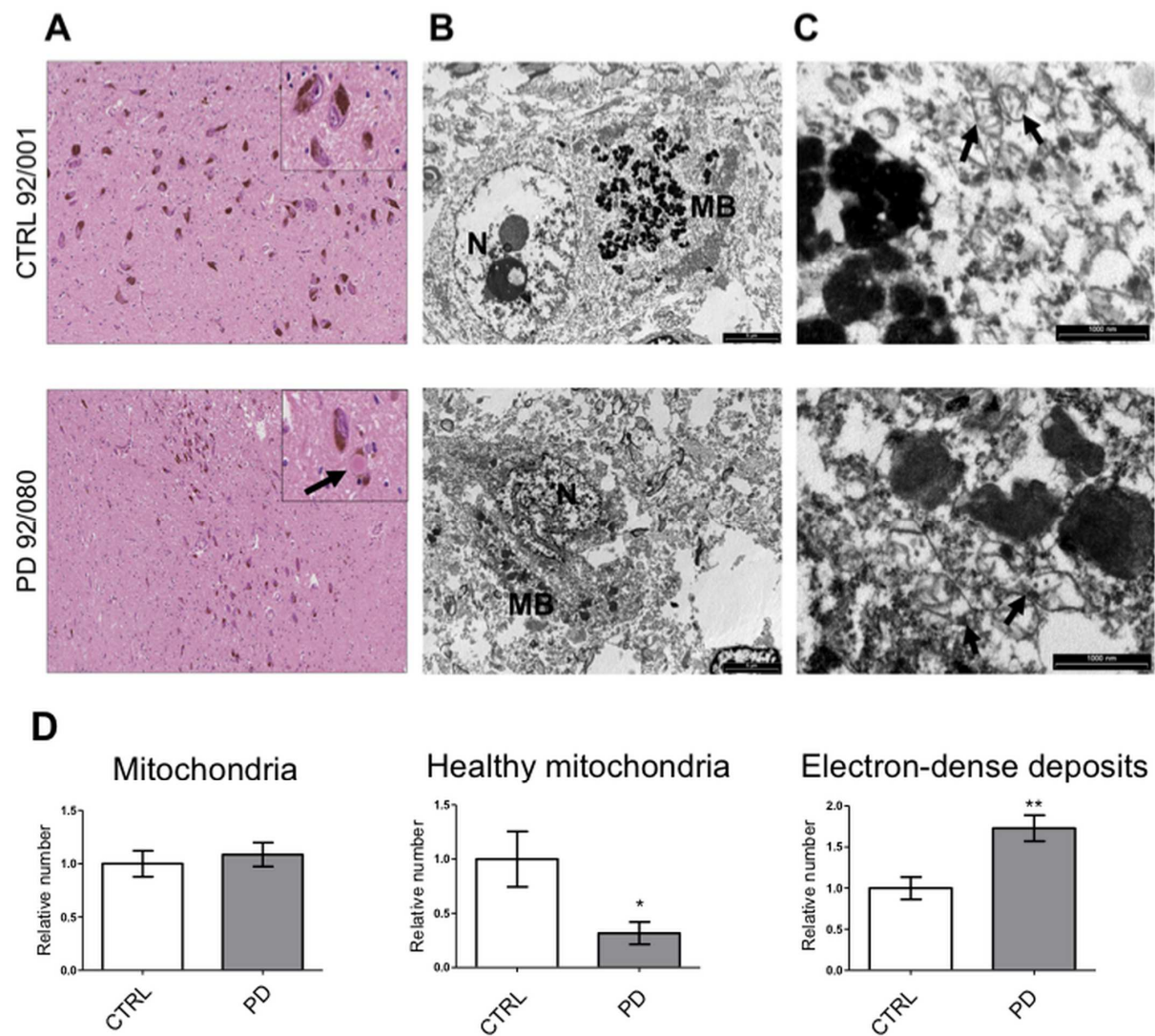


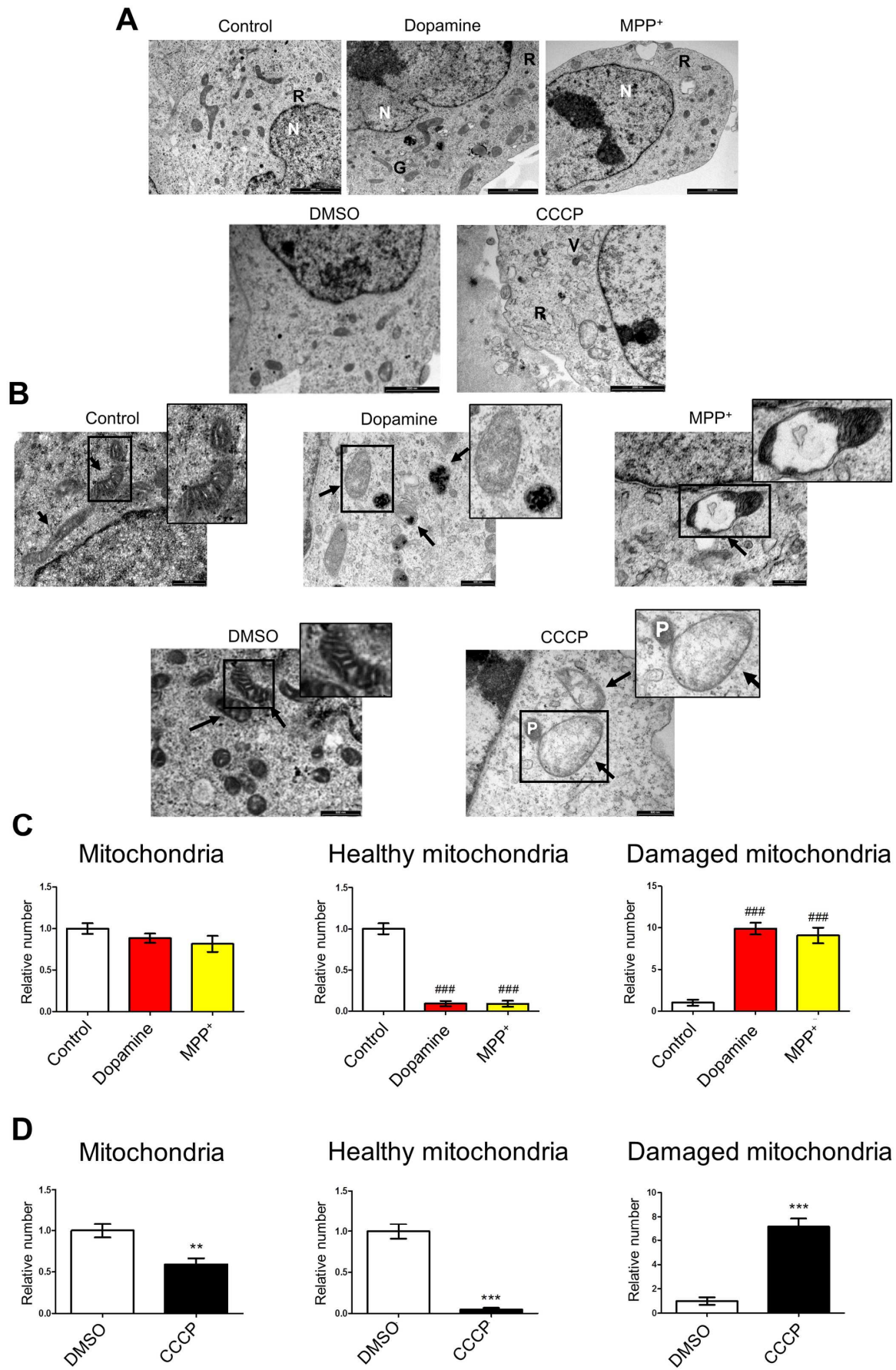
ACC











**Highlights**

- The inhibition of complex I by MPP<sup>+</sup> only partially reproduces PD mechanisms.
- Dopamine treatment better recapitulates mitochondrial impairment of PD.
- PINK1 does not accumulate in both sporadic PD patients and cellular models.
- Electron-dense deposits are present in mitochondria of PD patients.